Mathematical Modelling and Control

https://www.aimspress.com/journal/mmc

MMC, 4(3): 350–360.
DOI: 10.3934/mmc.2024028
Received: 14 June 2023
Revised: 13 April 2024
Accepted: 28 June 2024
Published: 11 September 2024

Research article

Analysis of amperometric biosensor utilizing synergistic substrates conversion: Akbari-Ganji's method

K. P. V. Preethi[1], **H. Alotaibi**[2] **and J. Visuvasam**[3,*]

[1] Department of Mathematics, Saiva Bhanu Kshatriya Colllege (Affiliated by Madurai Kamaraj University), Aruppukottai 626101, Virudhunagar, Tamil Nadu, India

[2] Department of Mathematics and Statistics, faculty of Science, Taif University, P. O. Box 11099, Taif 21944, Saudi Arabia

[3] Department of Mathematics, School of Engineering and Technology, Jain (Deemed-To-Be University), Bangalore-562 112, Karnataka, India

* **Correspondence:** Email: visuvasam135@gmail.com; Tel: +919629154552.

Abstract: The biological recognition of enzymes was the basis of enzyme-based chemical biosensors. It is essential for a biosensor to function under normal operating conditions so that enzymes can catalyze biochemical reactions. The mechanism of a modified enzyme-membrane electrode in a catalytic cycle was described using a mathematical model. The nonlinear terms associated with enzyme kinetics were presented in this model. The Akbari-Ganji's method (AGM) was used to calculate the semi-analytical expressions for species concentration and normalized current. For all possible values of the Thiele modulus, normalized surface concentration of the oxidized mediator, and normalized surface concentration of the substrate, a simple and approximate hyperbolic expression of concentrations of an oxidized mediator, substrate, and reduced mediator were derived. The numerical simulation was then verified using semi-analytical results. The numerical simulation and semi-analytical predictions agreed well with each other.

Keywords: mathematical modeling; nonlinear differential equations; Akbari-Ganji's method; numerical simulation; amperometric biosensor; immobilized enzyme

Abbreviations:

$[E_T]$: Total enzyme concentration, units: mM;
$[E_{OX}]$: Enzyme concentration of the oxygen, units: mM;
$[ES]$: Enzyme concentration of the substrate, units: mM;
$[E_{red}]$: Reduced enzyme concentration, units: mM;
$[Med_{OX}]$: Concentration of oxidized mediator at any position in the enzyme layer, units: mM;
$[Med_{red}]$: Concentration of reduced mediator at any position in the enzyme layer, units: $Molcm^{-3}$;
D_M: Diffusion coefficient of oxidized mediator, units: cm^2s^{-1};
D_S: Diffusion coefficient of substrate, units: cm^2s^{-1};
d: Thickness of the planar matrix, units: cm;
$[Med_{OX}]_b$: Oxidized mediator concentration at the enzyme layer electrode boundary, units: mM;
$[Med_{OX}]_\infty$: Oxidized mediator concentration in bulk solution, units: mM;
$[S]$: Concentration of substrate at any position in the enzyme layer, units: mM;
$[S]_b$: Concentration of substrate at any position in the enzyme layer electrode boundary, units: mM;
$[S]_\infty$: Substrate concentration in bulk solution, units: mM;
k_1, k_3, k_4: Rate constants, units: $M^{-1}s^{-1}$;
k_{-1}, k_2: Rate constants, units: s^{-1};
ϕ_O^2: Thiele modulus for the oxidized mediator, units: None

1. Introduction

The development of biosensing in recent decades has affected several fields, including environmental and biomedical monitoring. In modern biosensors, miniaturization, mass production, and simple transport processes are possible. Biological fluids constantly change, making biosensors an excellent real-time tool for monitoring these changes. Polymer membranes have been widely used as carriers for immobilizing enzymes in recent years [1]. Biocatalysts immobilized on membranes perform optimally. Catalytic reactions can be more selective toward desired products when substrate partitioning occurs at the membrane/fluid interphase (see [2]). A new approach to enzyme immobilization [3] based on molecular recognition has recently been used successfully for building chemically active membranes [4] as well as for building enzymatic biosensors. A great deal of effort has gone into developing biosensors with biologically sensitive components and transformers in the past decades, devices that have many possible applications [5]. Robeson demonstrated certain changes in membrane chemistry [6]. By enhancing the membrane area per unit volume, separation can be expedited by altering the membrane geometry. Recent research has identified increased surface area as a research priority for membranes [7].

Experiments were performed using a two-substrate model for enzyme electrodes incorporating nonlinear enzyme reactions [8]. Models of glucose oxidation electrodes have been developed using this approach [9]. When the mediators and natural co-substrates are both present in the assay solution, it has been found that the mediators cannot solely replace the co-substrate, so a three-substrate model is required. The calibration curve of the enzyme electrode is complex in these cases [10]. Although biosensors have been extensively tested experimentally, very few studies have focused on modeling or theoretical design. Efficient and productive biosensor design can be enhanced using a digital model [11–13]. The semi-analytical properties of biosensors have been optimized using mathematical models (see [14–17]). Biosensor models have been studied under steady-state [18, 19] and transient conditions [20, 21] using synergistic substrate conversion schemes.

A theoretical model for an enzyme-membrane amperometric oxidase electrode was recently presented by Loghambal et al. [22]. Novel enzyme electrodes were numerically analyzed in [23, 24]. Semi-analytical expressions of the substrate concentration for planar, cylindrical, and spherical particles under steady-state conditions were derived [25]. Lyons et al. [26] examined the problem of describing the transport and kinetics of catalytic reactions in a bounded region such as a conductive polymer-modified electrode.

Biological sensors have been assessed using electrochemical impedance spectroscopy, which is both nondestructive and sensitive to electrochemical properties [27–29]. An analysis of the influence of complex homogeneous and heterogeneous reactions on the sensor response was performed using mathematical models. A one-dimensional model for amperometric sensors was developed by Bartlett et al. and coworkers [30–32] based on the Michaelis-Menten approximation. Michaelis-Menten kinetics assumes a very large substrate concentration and that complex-forming reactions are equilibrated. A porous rotating disk electrode was recently analyzed by Visuvasam et al. [33]. The mathematical solution is semi-analytical, and more often, it is numerical. This method can be applied to various systems, and has been described in several publications [34–37]. This model can be understood better by reading [38–42] and its references.

This paper presents a semi-analytical solution for the model. By solving the system of nonlinear reaction-diffusion equations using Akbari-Ganji's (AGM) method (see [43, 44]), we can derive semi-analytical expressions for the substrate and oxidized and reduced mediator concentrations. These models provide information about the enzyme electrode mechanisms and their kinetics. These modeling results can be helpful for sensor design and optimization, and for determining how the electrode will react.

2. Mathematical formulation of the problem

The dimensionless nonlinear mass transport equation for this model was derived by Gooding and Hall [23]. A solid substrate encases the biological layer, and an

outer permeable electrode is in contact with the sample in the enzyme-membrane geometry. This model employs a permeable electrode to facilitate the penetration of the substrate and co-substrate into the enzyme layer, where it reduces to the form of a co-substrate that diffuses oxygen back to the electrode. In the presence of two oxidants, immobilized oxidase can be described by the following general reaction scheme [23]:

$$\mathrm{E_{ox}} + \mathrm{S} \underset{k_{-1}}{\overset{k_1}{\longrightarrow}} \mathrm{ES} \xrightarrow{k_2} \mathrm{E_{red}} + \mathrm{P}, \tag{2.1}$$

$$\mathrm{E_{red}} + \mathrm{O_2} \xrightarrow{k_3} \mathrm{E_{ox}} + \mathrm{H_2O_2}, \tag{2.2}$$

$$\mathrm{E_{red}} + \mathrm{Med_{ox}} \xrightarrow{k_4} \mathrm{E_{ox}} + \mathrm{Med_{red}} \tag{2.3}$$

with respect to the m^{th} reaction, k_m and k_{-m} represent the forward and backward rate constants, where $m = 1, 2, 3, \ldots,$ respectively. If $[E_T]$ is the total enzyme concentration in the matrix, then at all times

$$[E_T] = [E_{\mathrm{OX}}] + [\mathrm{ES}] + [E_{\mathrm{red}}], \tag{2.4}$$

where $[E_{OX}]$, $[ES]$, and $[E_{red}]$ are the oxidized mediator, enzyme-substrate complex, and reduced mediator enzyme concentrations, respectively. When a substrate diffuses into an enzyme layer at steady-state, its diffusion rate is equal to its reaction rate within the matrix. We consider a planar matrix of thickness $y = d$, where diffusion is only considered in the y-direction (see Figure 1).

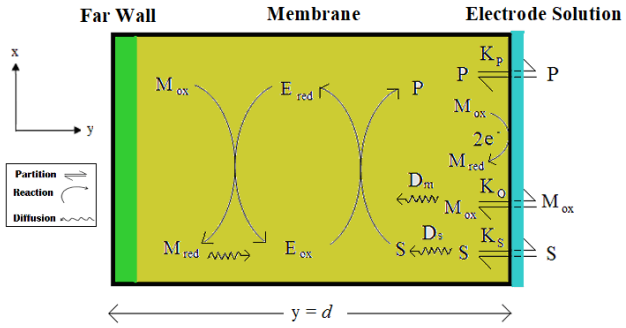

Figure 1. The geometry representation of enzyme-membrane electrode. The thicknesses of the layers are shown next to their boundaries [23].

On the enzyme electrode, the governing equations for the planar diffusion and reaction are as follows [23]:

$$\begin{aligned} D_M \frac{d^2\,[\mathrm{Med_{OX}}]}{\mathrm{dy}^2} &= k_4\,[E_{\mathrm{red}}]\,[\mathrm{Med_{OX}}] \\ &= [E_{\mathrm{OX}}]\,[S]\,\frac{k_2 k_1}{k_{-1}+k_2} \\ &= k_2\,[E_T]\left(\frac{\beta_S}{[S]} + \frac{\beta_O}{[\mathrm{Med_{OX}}]} + 1\right)^{-1}, \end{aligned} \tag{2.5}$$

$$\begin{aligned} D_S \frac{d^2[S]}{dy^2} &= k_1\,[E_{\mathrm{OX}}]\,[S] - k_{-1}[\mathrm{ES}] \\ &= [E_{\mathrm{OX}}]\,[S]\left(k_1 - \frac{k_{-1}k_1}{k_{-1}+k_2}\right) \\ &= k_2\,[E_T]\left(\frac{\beta_S}{[S]} + \frac{\beta_O}{[\mathrm{Med_{OX}}]} + 1\right)^{-1}, \end{aligned} \tag{2.6}$$

$$\begin{aligned} D_M \frac{d^2\,[\mathrm{Med_{red}}]}{\mathrm{dy}^2} &= -k_4\,[E_{\mathrm{red}}]\,[\mathrm{Med_{OX}}] \\ &= -k_2\,[E_T]\left(\frac{\beta_S}{[S]} + \frac{\beta_O}{[\mathrm{Med_{OX}}]} + 1\right)^{-1}, \end{aligned} \tag{2.7}$$

and from the above equations, we have

$$\begin{aligned} D_M \frac{d^2[\mathrm{MedOX}]}{dy^2} &= D_S \frac{d^2[S]}{\mathrm{dy}^2} \\ &= -D_M \frac{d^2\,[\mathrm{Med_{red}}]}{dy^2} \\ &= \frac{k_2\,[E_T]}{\frac{\beta S}{[S]} + \frac{\beta O}{[\mathrm{Med}^O\mathrm{OX}]} + 1}, \end{aligned} \tag{2.8}$$

where D_M and D_S are the diffusion coefficient of the mediator and substrate within the enzyme layer. $[\mathrm{Med_{OX}}]$, $[\mathrm{Med_{red}}]$, and $[S]$ are the concentration of oxidized, reduced mediators and the substrate within the enzyme layer.

$$\beta_S\ (= (k_{-1} + k_2)\,/k_1)$$

and

$$\beta_O = (k_2/k_4)$$

are the rate constants in dimensionless form.

The corresponding boundary conditions are the following: at the far wall, $y = 0$,

$$\frac{d\,[\mathrm{Med_{OX}}]}{\mathrm{dy}} = \frac{d[S]}{\mathrm{dy}} = \frac{d\,[\mathrm{Med_{red}}]}{\mathrm{dy}} = 0. \tag{2.9}$$

At the electrode, $y = d$,

$$\begin{aligned} [\mathrm{Med_{OX}}] = [\mathrm{Med_{OX}}]_b &= K_O\,[\mathrm{Med_{OX}}]_\infty, \\ [S] = [S]_b = K_S[S]_\infty,\ \ [\mathrm{Med_{red}}] &= 0, \end{aligned} \tag{2.10}$$

where $[\mathrm{Med_{OX}}]_b$ and $[S]_b$ are the bulk concentration of the oxidized mediator and substrate at the enzyme

layer electrode boundary. They are the bulk solution concentrations and are the equilibrium partition coefficients for the oxidized mediator and the substrate, respectively.

By defining the following dimensionless variables, we can reduce the nonlinear differential Eqs (2.5)–(2.7) to dimensionless form

$$F_O = \frac{[\mathrm{Med_{OX}}]}{[\mathrm{Med_{OX}}]_b},\ F_S = \frac{[\mathrm{S}]}{[\mathrm{S}]_b},\ F_R = \frac{[\mathrm{Med_{red}}]}{[\mathrm{Med_{red}}]_b},\ \chi = \frac{y}{d},$$
$$B_\mathrm{O} = \frac{[\mathrm{Med_{OX}}]_b}{\beta_\mathrm{O}},\ B_\mathrm{S} = \frac{[\mathrm{S}]_b}{\beta_\mathrm{S}},\ \phi_O^2 = \frac{d^2 k_2\,[E_T]}{D_M\,[\mathrm{Med_{OX}}]_b},$$
$$\mu_\mathrm{S} = \frac{D_M\,[\mathrm{Med_{Ox}}]_b}{D_S[\,\mathrm{S}]_b}, \tag{2.11}$$

where F_O, F_S, and F_R are the normalized concentration of the oxidized mediator, substrate, and reduced mediator, respectively, and χ is the normalized distance. B_O and B_S are the normalized surface concentration of the oxidized mediator and substrate. ϕ_O is the Thiele modulus for the oxidized mediator. Non-dimensionalized expressions for the oxidized mediator, substrate, and reduced mediator are as follows:

$$\frac{d^2F_O}{d\chi^2} = \phi_O^2\left[\frac{B_O B_S F_O F_S}{B_O F_O + B_S F_S + B_O B_S F_O F_S}\right], \tag{2.12}$$
$$\frac{d^2F_S}{d\chi^2} = \mu_S\phi_O^2\left[\frac{B_O B_S F_O F_S}{B_O F_O + B_S F_S + B_O B_S F_O F_S}\right], \tag{2.13}$$
$$\frac{d^2F_R}{d\chi^2} = -\phi_O^2\left[\frac{B_O B_S F_O F_S}{B_O F_O + B_S F_S + B_O B_S F_O F_S}\right]. \tag{2.14}$$

From the above equations, we obtain the following relations:

$$\begin{aligned}\frac{d^2F_O}{d\chi^2} &= \frac{1}{\mu_S}\frac{d^2F_S}{d\chi^2}\\ &= -\frac{d^2F_R}{d\chi^2}\\ &= \phi_O^2\left[\frac{B_O B_S F_O F_S}{B_O F_O + B_S F_S + B_O B_S F_O F_S}\right].\end{aligned} \tag{2.15}$$

Corresponding boundary conditions are given by:

$$F_O' = 0,\ F_S' = 0,\ F_R' = 0 \text{ at } \chi = 0, \tag{2.16}$$
$$F_O = 1,\ F_S = 1,\ F_R = 0 \text{ at } \chi = 1. \tag{2.17}$$

From Eq (2.14), we get

$$\frac{d^2F_O}{d\chi^2} = \frac{1}{\mu_S}\frac{d^2F_S}{d\chi^2} \tag{2.18}$$

and

$$\frac{d^2F_R}{d\chi^2} = -\frac{1}{\mu_S}\frac{d^2F_S}{d\chi^2}. \tag{2.19}$$

Solving Eqs (2.18) and (2.19) we get

$$F_O(\chi) = \frac{1}{\mu_S}\left(F_S(\chi) - 1\right) + 1, \tag{2.20}$$
$$F_R(\chi) = \frac{1}{\mu_S}\left(1 - F_S(\chi)\right). \tag{2.21}$$

The following expression gives the normalized current response:

$$I = -\left(\frac{dF_R}{d\chi}\right)_{\chi=1}. \tag{2.22}$$

3. Approximate analytical expressions for the oxidized mediator, substrate, and reduced mediator using AGM

AGM [45–49] was used to solve the boundary value problem and its associated boundary conditions represented by Eqs (2.12)–(2.17), which has a minimum number of unknowns. This is an appropriate and simple method for nonlinear differential equations [50]. This is a particular case of the exponential function method proposed by He et al. [51]. Using this method, a general semi-analytical expression for the normalized concentrations can be obtained as follows:

$$F_S(\chi) \approx \frac{\cosh(b\chi)}{\cosh(b)}, \tag{3.1}$$
$$F_O(\chi) \approx 1 - \frac{1}{\mu_S}\left(1 - \frac{\cosh(b\chi)}{\cosh(b)}\right), \tag{3.2}$$
$$F_R(\chi) \approx \frac{1}{\mu_S}\left(1 - \frac{\cosh(b\chi)}{\cosh(b)}\right), \tag{3.3}$$

where

$$b = \phi_0\sqrt{\frac{\mu_S B_O B_S}{B_O + B_S + B_O B_S}}. \tag{3.4}$$

From these relations, the following current response formula is derived:

$$I = -\left(\frac{dF_R}{d\chi}\right)_{\chi=1} = \frac{b}{\mu_S}\tanh(b). \tag{3.5}$$

4. Previous analytical results for concentration for the oxidized mediator, substrate, and reduced mediator [52]

Loghambal et al. [52] derived the approximate semi-analytical expressions for the concentration for the oxidized

mediator, substrate, and reduced mediator using the adomian decomposition method

$$F_O(\chi) \approx 1 + \frac{\phi_0^2 B_O B_S}{2(B_O + B_S + B_O B_S)}(5w_1 - 1 + (1 - 6w_1)\chi^2 + w_1\chi^4), \tag{4.1}$$

$$F_S(\chi) \approx \mu_S(F_O(\chi) - 1) + 1, \tag{4.2}$$

$$F_R(\chi) \approx 1 - F_O(\chi). \tag{4.3}$$

The normalized current becomes

$$I = \frac{\phi_O^2 B_O B_S (1 - 4w_1)}{B_O + B_S + B_O B_S}, \tag{4.4}$$

where

$$w_1 = \phi_O^2 B_O B_S (B_S + B_O \mu_S)/12(B_O + B_S + B_O B_S)^2.$$

5. Numerical simulation

Numerical methods are used to solve the nonlinear differential Eqs (2.12)–(2.14). A numerical solution of the nonlinear differential Eqs (2.12)–(2.14) has been performed via MATLAB. Comparing our numerical solutions with our analytical results is shown in Figures 2–4 regarding species concentrations. The numerical solution, which is shown in Figures 2–4, yields a satisfactory result when compared to the AGM.

6. Discussion

Equations (3.1)–(3.3) provide semi-analytical expressions of the concentrations of the substrate, oxygen, and reduced mediators that are obtained by using AGM with the normalized current given in Eq (3.5). Figure 2a–c depicts the normalized steady-state concentrations of species obtained using Eq (2.12)–(2.14) for various values of ϕ_0 and for some fixed values of μ_S, B_O, and B_S. The concentration is uniform when $\phi_0 \leq 1$ for all species. Figure 2a,b shows that for some fixed values of other parameters μ_S, B_O, and B_S, the normalized concentrations of the oxidized mediator and substrate decrease with the increasing Thiele modulus. In contrast, this modulus has an opposite effect on the normalized concentrations of the reduced mediator for some fixed values of the μ_S, B_O and B_S as shown in Figure 2c.

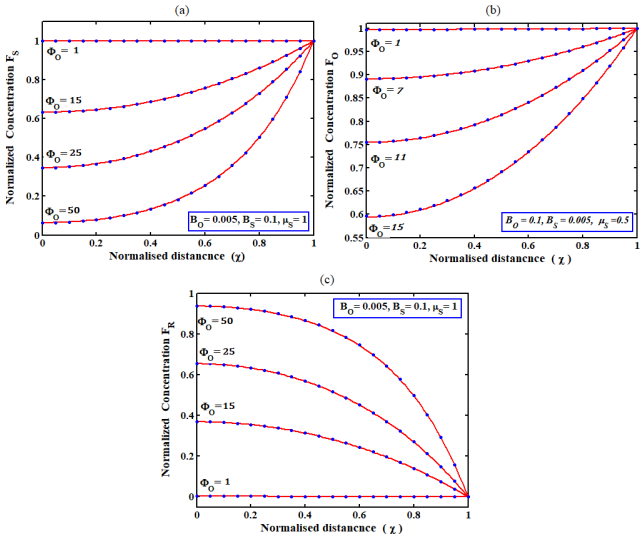

Figure 2. Comparison of the concentration profile with simulation results for various values of normalized parmeter ϕ_0: (a) substrate (Eq (3.1)); (b) oxidized mediator (Eq (3.2)); (c) reduced mediator (Eq (3.3)). Solid line represents the semi-analytical result and (...) represents the numerical result.

Figure 3a–c illustrates the normalized concentrations of substrates, the oxidized mediator and reduced mediator, versus the dimensionless distance, respectively. Figure 3a,b shows that, for some fixed values of the parameters μ_S, ϕ_0, and B_S concentrations of substrates and the oxidized mediator decrease as B_O increases. Figure 3c illustrates that for some constant measurements of the parameters μ_S, ϕ_0, and B_S, the normalized surface concentrations of the reduced mediator increase as B_O increases.

According to Eqs (2.12)–(2.14), the normalized steady-state concentrations of substrate and various mediator species can be determined for various values of B_S as shown in Figure 4a–c. We conclude that when the dimensionless parameter B_S increases, the concentrations of substrate and oxidized mediator decrease for some fixed values of the parameters μ_S, ϕ_0, and B_O in Figure 4a,b. In Figure 4c, it can be seen that the influence of the increasing dimensionless parameter B_S can result in normalized concentrations of the mediator increasing, even when the other parameter is at fixed values.

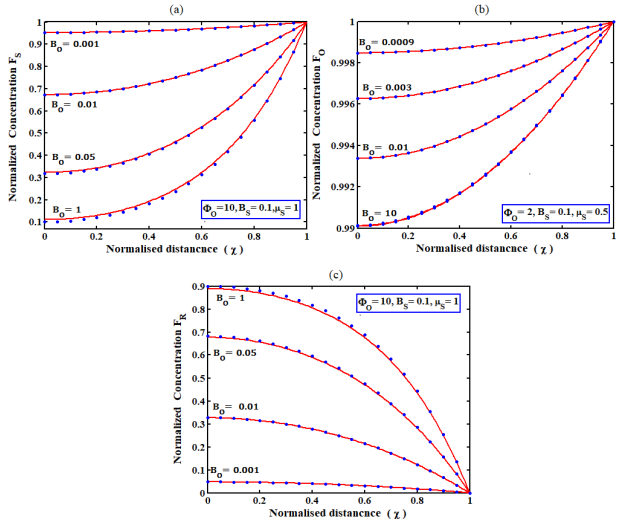

Figure 3. Comparison of the concentration profile with simulation results for various values of normalized parmeter B_{O}: (a) substrate (Eq (3.1)); (b) oxidized mediator (Eq (3.2)); (c) reduced mediator (Eq (3.3)). Solid line represents the semi-analytical result and (. . .) represents the numerical result.

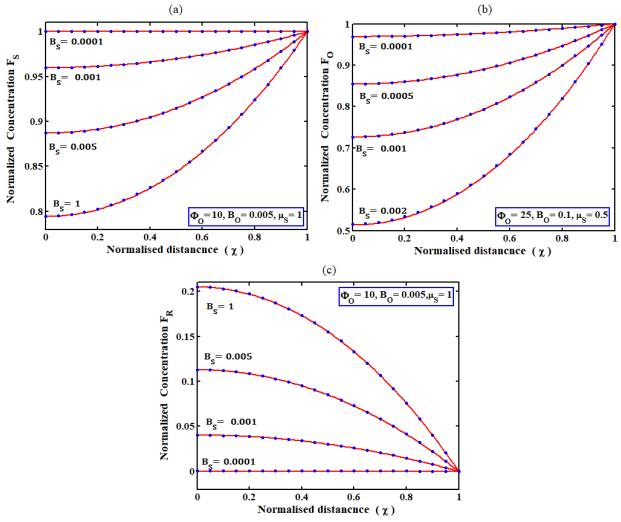

Figure 4. Comparison of the concentration profile with simulation results for various values of normalized parmeter B_{S}: (a) substrate (Eq (3.1)); (b) oxidized mediator (Eq (3.2)); (c) reduced mediator (Eq (3.3)). Solid line represents the semi-analytical result and (. . .) represents the numerical result.

Figure 5a–c illustrates the normalized concentrations of substrates, oxidized mediator, and reduced mediator versus the dimensionless distance χ, respectively. Figure 5a,b shows that, for some fixed values of the parameters ϕ_0, B_{S}, and B_{O}, concentrations of substrates and reduced mediator decrease as μ_{S} increases. Figure 5c illustrates that for some constant measurements of the parameters ϕ_0, B_{S}, and B_{O}, the normalized surface concentrations of the oxidized mediator increase as μ_{S} increases.

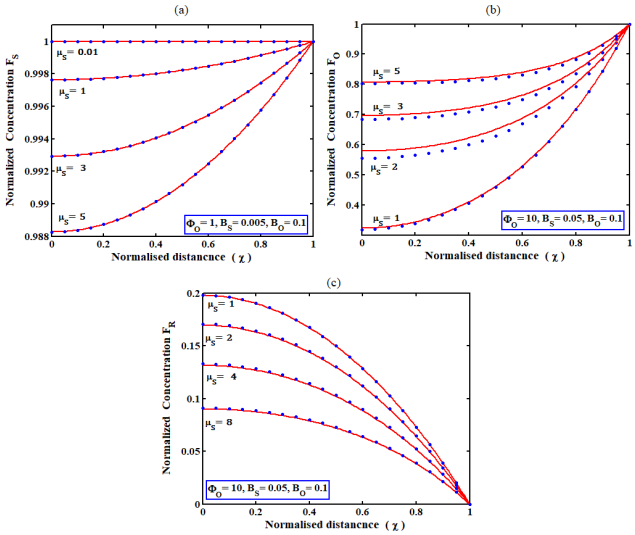

Figure 5. Comparison of the concentration profile with simulation results for various values of normalized parmeter μ_{S}: (a) substrate (Eq (3.1)); (b) oxidized mediator (Eq (3.2)); (c) reduced mediator (Eq (3.3)). Solid line represents the semi-analytical result and (. . .) represents the numerical result.

The effect of the various parameters on the current in the three-dimensional is displayed in Figure 6a–c. The dependencies of the steady-state current I on the concentration of the substrate, oxygen, and reduced mediators versus the Thiele modulus are displayed in Figure 6. It is noticed from these figures that the steady-state current increases as the values of the parameters μ_{S}, ϕ_0, B_{O}, and B_{S} increase. The proposed empirical concentration models are compared with the corresponding numerical data in Tables 1 and 2.

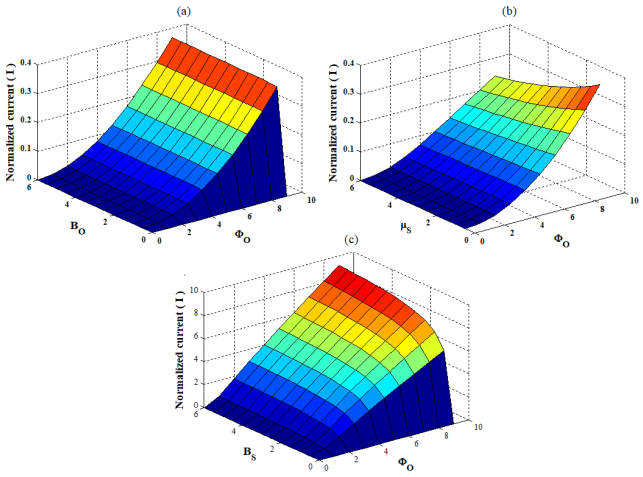

Figure 6. Three-dimensional plot for normalized current I versus Thiele modulus and (a) B_{O} (b)μ_{S} (c) B_{S} using (3.5).

Table 1. Comparison of normalized current I in Eq (3.5) and previous results in Eq (4.4) with simulation results when $B_O = 0.1, B_S = 0.01$, and $\mu_S = 0.05$ and for various values of parameter (ϕ_O^2) Thiele module.

ϕ_0^2	Previous results in Eq (4.4)	Our results in Eq (3.5)	Numerical
1	0.009	0.009	0.0090
25	0.223	0.224	0.2230
50	0.441	0.447	0.4410
75	0.655	0.668	0.6520
100	0.864	0.887	0.8380

7. Conclusions

An amperometric enzyme-based biosensor combines chemistry, biology, electrochemistry, materials science, polymer synthesis, enzymology, and electrochemistry to provide a powerful analytical tool.

Our main goal was to develop a biosensor that responds to oxidase linked tests independently of biorecognition matrix thickness for oxidase linked tests. The mathematical models (2.12)–(2.14) of the biosensor utilizing the synergistic scheme of substrates conversion can be successfully used to investigate the peculiarities of the biosensor response and sensitivity at steady as well as at transition state. In the amperometric biosensor system, a nonlinear differential equation was used to determine the semi-analytical solution of the species concentration. Using the AGM, an approximate general semi-analytical expression for the concentration of substrate, mediator and current of amperometric biosensor at the enzyme-membrane electrode geometry is derived for all values of parameters ϕ_O^2, B_O, and B_S. The effects of these parameters on the concentration and effectiveness were also explored. The results were satisfactory compared to those of the numerical simulation. It is possible to determine the qualitative behavior of biosensors by using this hypothetical model. Furthermore, the results of this study provide an option for extending this method to measure substrate concentrations and diffusion currents. As the reciprocal of the squares of the Thiele modulus decreases, the current density increases. The results of this study can be used to optimize and design biosensors.

Acknowledgments

The authors extend their appreciation to Taif University, Saudi Arabia, for supporting this work through project number (TU-DSPP-2024-92).

Conflict of interest

All authors declare no conflicts of interest in this paper.

References

1. E. Simon, C. M. Halliwell, C. S. Toh, A. E. G. Cass, P. N. Bartlett, Immobilisation of enzymes on poly(aniline)-poly(anion) composite films. Preparation of bioanodes for biofuel cell applications, *Bioelectrochemistry*, **55** (2002), 13–15. https://doi.org/10.1016/s1567-5394(01)00160-8
2. M. D. Trevan, *Immobilised enzymes*, 2 Eds., Wiley, 1989.
3. Q. T. Nguyen, Z. Ping, T. Nguyen, P. Rigal, Simple method for immobilization of bio-macromolecules onto membranes of different types, *J. Membr. Sci.*, **213** (2003), 85–95. https://doi.org/10.1016/S0376-7388(02)00515-X

Table 2. Comparison of concentration of oxidized mediator in Eq (3.1) and previous in Eq (4.1) with simulation results when $B_O = 0.1$, $B_S = 0.01$, and $\mu_S = 0.05$, and for various values of parameter (ϕ_O^2) Thiele module.

$\phi_O^2 = 0.01$						$\phi_O^2 = 1$					
χ	Previous results in Eq (4.1)	Our results in Eq (3.1)	Numerical	Error in Eq (4.1)	Error for Eq (3.1)	χ	Previous results in Eq (4.1)	Our results in Eq (3.1)	Numerical	Error in Eq (4.1)	Error for Eq (3.1)
0	0.9999	0.9999	1	0.01	0.01	0	0.9955	0.9955	0.9955	0.00	0.00
0.2	0.9999	0.9999	1	0.01	0.01	0.2	0.9957	0.9957	0.9957	0.00	0.00
0.4	0.9999	0.9999	1	0.01	0.01	0.4	0.9962	0.9962	0.9962	0.00	0.00
0.6	0.9999	0.9999	1	0.01	0.01	0.6	0.9971	0.9971	0.9971	0.00	0.00
0.8	0.9999	0.9999	1	0.01	0.01	0.8	0.9984	0.9984	0.9984	0.00	0.00
1	1	1	1	0	0	1	1	1	1	0.00	0.00
Average deviation				0.05	0.05	Average deviation				0.00	0.00
$\phi_O^2 = 25$						$\phi_O^2 = 100$					
χ	Previous results in Eq (4.1)	Our results in Eq (3.1)	Numerical	Error in Eq (4.1)	Error for Eq (3.1)	χ	Previous results in Eq (4.1)	Our results in Eq (3.1)	Numerical	Error in Eq (4.1)	Error for Eq (3.1)
0	0.8889	0.8889	0.8889	0.00	0.00	0	0.5801	0.5795	0.5773	0.46	0.45
0.2	0.8933	0.8923	0.8923	0.00	0.00	0.2	0.5965	0.5966	0.5939	0.43	0.42
0.4	0.9066	0.9058	0.9060	0.00	0.02	0.4	0.6462	0.6463	0.6440	0.34	0.34
0.6	0.9288	0.9282	0.9282	0.00	0.00	0.6	0.7295	0.7296	0.7279	0.22	0.22
0.8	0.9599	0.9596	0.9599	0.00	0.03	0.8	0.9484	0.9485	0.8479	0.85	0.83
1	1	1	1	0.00	0.00	1	1	1	1	0.00	0.00
Average deviation				0.00	0.05	Average deviation				0.38	0.37

4. A. Bhardwaj, L. Jinbo, K. Glauner, S. Ganapathi, D. Bhattacharyya, D. A. Butterfield, Biofunctional membranes: an EPR study of active site structure and stability of papain non-covalently immobilized on the surface of modified poly(ether)sulfone membranes through the avidin-biotin linkage, *J. Membr. Sci.*, **119** (1996), 241–252. https://doi.org/10.1016/0376-7388(96)00124-X

5. G. G. Guilbault, Immobilised enzymes and cells, In: K. Mosbach, *Methods in enzymology*, Academic Press, 1988.

6. L. M. Robeson, Correlation of separation factor versus permeability for polymericmembranes, *J. Membr. Sci.*, **62** (1991), 165–185. https://doi.org/10.1016/0376-7388(91)80060-J

7. A. M. Gronda, S. Buechel, E. L. Cussler, Mass transfer in corrugated membranes, *J. Membr. Sci.*, **165** (2000), 177–187. https://doi.org/10.1016/S0376-7388(99)00230-6

8. J. J. Gooding, E. A. H. Hall, Parameters in the design of oxygen detecting oxidase enzyme electrodes, *Electroanalysis*, **8** (1996), 407–413. https://doi.org/10.1002/elan.1140080502

9. S. Turmanova, A. Trifonov, O. Kalaijiev, G. Kostov, Radiation grafting of acrylic acid onto polytetrafluoroethylene films for glucose oxidase immobilization and its application in membrane biosensor, *J. Membr. Sci.*, **127** (1997), 1–7. https://doi.org/10.1016/S0376-7388(96)00277-3

10. T. Y. Ohara, R. Rajagopalan, A. Hellcr, Research article glucose electrodes based on cross-linked bis(2,2'-bipyridine) chloroosmium(+/2+) complexed poly(1-vinylimidazole) films, *Anal. Chem.*, **65** (1993), 3512–3517. https://doi.org/10.1021/ac00071a031

11. J. I. R. de Corcuera, R. P. Cavalieri, J. R. Powers, J. Tang, Amperometric enzyme biosensor optimization using mathematical modeling, *Proceedings of the 2004 ASAE/CSAE Annual International Meeting*, 2004. https://doi.org/10.13031/2013.17018

12. O. V. Klymenko, C. Amatore, W. Sun, Y. Zhou, Z. Tian, I. Svir, Theory and computational study of electrophoretic ion separation and focusing in microfluidic channels, *Nonlinear Anal.*, **17** (2012), 431–447. https://doi.org/10.15388/NA.17.4.14049

13. Y. Nishio, S. Uno, K. Nakazato, Three-dimensional simulation of DNA sensing by ion-sensitive field-effect transistor: optimization of DNA position and orientation, *Jpn. J. Appl. Phys.*, **52** (2013), 04CL01. https://doi.org/10.7567/JJAP.52.04CL01

14. T. Schulmeister, D. Pfeiffer, Mathematical modelling of amperometric enzyme electrodes with perforated membranes, *Biosens. Bioelectron.*, **8** (1993), 75. https://doi.org/10.1016/0956-5663(93)80055-T

15. W. E. Morf, P. D. van der Wal, E. Pretsch, N. F. de Rooij, Theoretical treatment and numerical simulation of potentiometric and amperometric enzyme electrodes and of enzyme reactors. Part 1: steady-state concentration profiles, fluxes, and responses, *J. Electroanal. Chem.*, **657** (2011), 1–12. https://doi.org/10.1016/j.jelechem.2011.02.007

16. R. Baronas, F. Ivanauskas, J. Kulys, *Mathematical modeling of biosensors*, Springer, 2010. https://doi.org/10.1007/978-90-481-3243-0

17. R. A. Croce, S. Vaddiraju, F. Papadimitrakopoulos, F. C. Jain, Theoretical analysis of the performance of glucose sensors with layer-by-layer assembled outer membranes, *Sensors*, **12** (2012), 13402. https://doi.org/10.3390/s121013402

18. A. J. Bergren, M. D. Porter, The characteristics of selective heterogeneous electron transfer for optimization of redox recycling amplification systems, *J. Math. Chem.*, **591** (2006), 189–200. https://doi.org/10.1016/j.jelechem.2006.04.005

19. J. Kulys, Z. Dapkunas, The effectiveness of synergistic enzymatic reaction with limited mediator stability, *Nonlinear Anal.*, **12** (2007), 495–501. https://doi.org/10.15388/NA.2007.12.4.14680

20. J. Kulys, L. Tetianec, Synergistic substrates determination with biosensors, *Biosens. Bioelectron.*, **21** (2005), 152–158. https://doi.org/10.1016/j.bios.2004.08.013

21. E. Gaidamauskaite, R. Baronas, J. Kulys, Modelling synergistic action of laccasebased biosensor utilizing simultaneous substrates conversion, *J. Math. Chem.*, **49** (2011), 1573–1586. https://doi.org/10.1007/s10910-011-9844-1

22. S. Loghambal, L. Rajendran, Mathematical modeling in amperometric oxidase enzyme-membrane electrodes, *J. Membr. Sci.*, **373** (2011), 20–28. https://doi.org/10.1016/j.memsci.2011.02.033

23. J. J. Gooding, E. A. H. Hall, Practical and theoretical evaluation of an alternative geometry enzyme electrode, *J. Electroanal. Chem.*, **417** (1996), 25–33. https://doi.org/10.1016/S0022-0728(96)04752-3

24. G. Adomian, Convergent series solution of nonlinear equations, *J. Comput. Appl. Math.*, **11** (1984), 225–230. https://doi.org/10.1016/0377-0427(84)90022-0

25. M. C. Devi, P. Pirabaharan, L. Rajendran, M. Abukhaled, An efcient method for fnding analytical expressions of substrate concentrations for diferent particles in an immobilized enzyme system, *React. Kinet. Mech. Cat.*, **130** (2020), 35–53. https://doi.org/10.1007/s11144-020-01757-0

26. M. E. G. Lyons, Transport and kinetics in electrocatalytic thin film conducting polymer biosensors: bounded diffusion with Michaelis-Menten kinetics incorporating general inhibition effects, *Int. J. Electrochem. Sci.*, **15** (2020), 6060–6090. https://doi.org/10.20964/2020.07.01

27. K. J. Otto, M. D. Johnson, D. R. Kipke, Voltage pulses change neural interface properties and improve unit recordings with chronically implanted microelectrodes, *IEEE Trans. Biomed. Eng.*, **53**, (2006), 333–340. https://doi.org/10.1109/tbme.2005.862530

28. E. Katz, I. Willner, Probing biomolecular interactions at conductive and semi conductive surfaces by impedance spectroscopy: routes to impedimetric immunosensors, dna-sensors, and enzyme biosensors, *Electroanalysis*, **15** (2003), 913–947. https://doi.org/10.1002/elan.200390114

29. V. Sankar, E. Patrick, R. Dieme, J. C. Sanchez, A. Prasad, T. Nishida, Electrode impedance analysis of chronic tungsten microwire neural implants: understanding abiotic vs. biotic contributions, *Front. Neuroeng.*, **7** (2014), 00013. https://doi.org/10.3389/fneng.2014.00013

30. W. Albery, P. N. Bartlett, B. J. Driscoll, R. Lennox, Amperometric enzyme electrodes: Part 5. The homogeneous mediated mechanism, *J. Electroanal. Chem.*, **323** (1992), 77–102. https://doi.org/10.1016/0022-0728(92)80004-N

31. P. Bartlett, R. Whitaker, Electrochemical immobilisation of enzymes: Part I. Theory, *J. Electroanal. Chem. Interfacial Electrochem.*, **224** (1992), 27–35. https://doi.org/10.1016/0022-0728(87)85081-7

32. P. Bartlett, K. Pratt, Modelling of processes in enzyme electrodes, *Biosens. Bioelectron.*, **8** (1993), 451–462. https://doi.org/10.1016/0956-5663(93)80030-S

33. J. Visuvasam, A. Hammad, Analysis of Von Kármán swirling flows due to a porous rotating disk electrode, *Micromachines*, **14** (2023), 582. https://doi.org/10.3390/mi14030582

34. J. Galceran, S. Taylor, P. Bartlett, Modelling the steady-state current at the inlaid disc microelectrode for homogeneous mediated enzyme catalysed reactions, *J. Electroanal. Chem.*, **506** (2001), 65–81. https://doi.org/10.1016/S0022-0728(01)00503-4

35. M. Shoaib, G. Zubair, K. S. Nisar, M. A. Z. Raja, M. I. Khan, R. J. P. Gowda, et al., Ohmic heating effects and entropy generation for nanofluidic system of Ree-Eyring fluid: intelligent computing paradigm, *Int. Commun. Heat Mass Transfer*, **129** (2021), 105683. https://doi.org/10.1016/j.icheatmasstransfer.2021.105683

36. Y. Xu, S. Faisal, K. M. Ijaz, R. N. Kumar, R. J. P. Gowda, B. C. Prasannakumara, et al., New modeling and analytical solution of fourth grade (non-Newtonian) fluid by a stretchable magnetized Riga device, *Int. J. Mod. Phys. C*, **33** (2022), 2250013. https://doi.org/10.1142/S0129183122500139

37. M. Sunitha, F. Gamaoun, A. Abdulrahman, N. S. Malagi, S. Singh, R. J. Gowda, et al., An efficient analytical approach with novel integral transform to study the two-dimensional solute transport problem, *Ain Shams Eng. J.*, **14** (2022), 101878. https://doi.org/10.1016/j.asej.2022.101878

38. R. J. P. Gowda, R. Naveenkumar, J. K. Madhukesh, B. C. Prasannakumara, R. S. R. Gorla, Theoretical analysis of SWCNT-MWCNT/H2O hybrid flow over an upward/downward moving rotating disk, *Proc. Inst. Mech. Eng. Part N*, **235** (2021), 97–106. https://doi.org/10.1177/2397791420980282

39. O. A. Bég, U. S. Mahabaleshwar, M. M. Rashidi, N. Rahimzadeh, J. L. C. Sosa, I. Sarris, et al., Homotopy analysis of magnetohydrodynamic convection flow in manufacture of a viscoelastic fabric for space applications, *Int. J. Appl. Math. Mech.*, **10** (2014), 9–49.

40. G. Sowmya, R. S. V. Kumar, M. D. Alsulami, B. C. Prasannakumara, Thermal stress and temperature distribution of an annular fin with variable temperature-dependent thermal properties and magnetic field using DTM-Pade approximant, *Waves Random Complex Media*, 2022. https://doi.org/10.1080/17455030.2022.2039421

41. K. M. Dharmalingam, M. Veeramuni, Akbari-Ganji's method (AGM) for solving non-linear reaction-diffusion equation in the electroactive polymer film, *J. Electroanal. Chem.*, **844** (2019), 1–5. https://doi.org/10.1016/j.jelechem.2019.04.061

42. M. R. Akbari, D. D. Ganji, A. R. Goltabar, S. H. H. Kachapi, Analyzing the nonlinear vibrational wave differential equation for the simplified model of tower cranes by algebraic method, *Front. Mech. Eng.*, **9** (2014), 58–70. https://doi.org/10.1016/j.ijoes.2023.100113

43. R. Swaminathan, M. C. Devi, L. Rajendran, K. Venugopal, Sensitivity and resistance of amperometric biosensors in substrate inhibition processes, *J. Electroanal. Chem.*, **895** (2021), 115527. https://doi.org/10.1016/j.jelechem.2021.115527

44. A. Reena, S. G. Karpagavalli, L. Rajendran, B. Manimegalai, R. Swaminathan, Theoretical analysis of putrescine enzymatic biosensor with optical oxygen transducer in sensitive layer using Akbari-Ganji method, *Int. J. Electrochem. Sci.*, **18** (2023), 100113. https://doi.org/10.1016/j.ijoes.2023.100113

45. M. R. Akbari, D. D. Ganji, M. Nimafar, A. R. Ahmadi, Significant progress in solution of nonlinear equations at displacement of structure and heat transfer extended surface by new AGM approach, *Front. Mech. Eng.*, **9** (2014), 390–401. https://doi.org/10.1007/s11465-014-0313-y

46. B. Manimegalai, M. E. G. Lyons, L. Rajendran, A kinetic model for amperometric immobilized enzymes at planar, cylindrical and spherical electrodes: the Akbari-Ganji method, *J. Electroanal. Chem.*, **880** (2021), 114921. https://doi.org/10.1016/j.jelechem.2020.114921

47. R. Shanthi, D. M. Chitra, M. Abukhaled, M. E. G. Lyons, L. Rajendran, Mathematical modeling of pH-based potentiometric biosensor using Akbari-Ganji method, *Int. J. Electrochem. Sci.*, **17** (2022), 220349. https://doi.org/10.20964/2022.03.48

48. K. Ranjani, R. Swaminathan, S. G. Karpagavalli, Mathematical modelling of a mono-enzyme dual amperometric biosensor for enzyme-catalyzed reactions using homotopy analysis and Akbari-Ganji methods, *Int. J. Electrochem. Sci.*, **18** (2023), 100220. https://doi.org/10.1016/j.ijoes.2023.100220

49. M. A. Attar, M. Roshani, K. Hosseinzadeh, D. D. Ganji, Analytical solution of fractional differential equations by Akbari-Ganji's method, *Partial Differ. Equations Appl. Math.*, **6** (2022), 100450. https://doi.org/10.1016/j.padiff.2022.100450

50. J. Visuvasam, A. Meena, L. Rajendran, New analytical method for solving nonlinear equation in rotating disk electrodes for second order ECE reactions, *J. Electroanal. Chem.*, **869** (2020), 114106. https://doi.org/10.1016/j.jelechem.2020.114106

51. J. He, A simple approach to one-dimensional convection-diffusion equation and its fractional modification for E reaction arising in rotating disk electrode, *J. Electroanal. Chem.*, **854** (2019), 113565. https://doi.org/10.1016/j.jelechem.2019.113565

52. L. Shunmugham, L. Rajendran, Analytical expressions for steady-state concentrations of substrate and oxidized and reduced mediator in an amperometric biosensor, *Int. J. Electrochem.*, 2013, 812856. https://doi.org/10.1155/2013/812856

AIMS Press